Environmental Processes (2025) 12:54
https://doi.org/10.1007/s40710-025-00797-9

RESEARCH

Application of a 2D Hydrodynamic Numerical Model for Heavy Precipitation-Induced Soil Erosion

Rebecca Hinsberger[1,2] · **Alpaslan Yörük**[2,3]

Received: 7 May 2025 / Accepted: 5 September 2025

Abstract

Soil erosion, particularly when intensified by heavy precipitation, is a natural process and a persistent challenge in agricultural management. To date, this problem has been addressed using existing erosion models. However, these models often rely on simplified hydraulic approaches, whereas two-dimensional (2D) hydrodynamic numerical models are state-of-the-art for overland flow simulations. In this study, the combination of a 2D model and a soil erosion approach allowed for a more precise consideration of the hydraulics. The Govers approach was used with the 2D HydroAS model and evaluated using experimental plot data and naturally occurring field-scale erosion data, sourced from the literature. Results indicate that the combined model simulated sheet erosion and produced reasonable estimates for small rills using the Govers transport capacity approach. However, larger rills require calibration of this method. Additionally, the resolution of the digital elevation model (0.25 m) used as the basis for the simulation was of great importance to avoid overestimating smaller rills. Sensitivity analysis revealed that these smaller rills were particularly influenced by the input grain diameter and surface roughness. Comparisons with other erosion models underscore that incorporating an improved hydraulic approach and adapting the topography at each simulation time step enhances estimation of the spatial distribution and quantity of erosion of the rills. Knowledge about the occurrence and quantification of rill erosion can help planners develop geoecological solutions for flooding and erosion.

Highlights

- A 2D hydrodynamic numerical model was combined with a soil erosion approach.
- Accurate hydraulic calculations improve estimates of rill erosion quantity.
- Accurate hydraulic calculations improve the spatial representation of rills.
- The Govers transport capacity approach is suitable for modeling soil erosion.
- The resolution of the DEM input significantly influences model outcomes.

Keywords Flash flood simulation · Rain-on-grid modeling · HydroAS GS · Govers approach · Rill erosion

Extended author information available on the last page of the article

Published online: 14 October 2025

1 Introduction

Heavy precipitation events with increasing rainfall erosivity occur frequently, leading to flash floods that adversely affect human settlements and infrastructure (IPCC 2021; Nunes and Nearing 2011). Beyond the risk of water damage, soil loss can cause on-site and off-site damage. According to Parkin et al. (2008), a few heavy precipitation events account for the majority of erosion. Flash floods are defined as overland flow with shallow water depths and steep slopes. On these slopes, there is high sediment concentration resulting from soil erosion (Dugan et al. 2024; Govers 1990; Semwal et al. 2017).

Several models are currently available to simulate overland flow and erosion. These range from empirical models, such as the Universal Soil Loss Equation (USLE) (Wischmeier and Smith 1978), to process-oriented models like the Water Erosion Prediction Project (WEPP) (Laflen et al. 1991), the European Soil Erosion Model (EUROSEM) (Morgan et al. 1998a), the Areal Nonpoint Source Watershed Environment Response Simulation (ANSWERS) (Beasley et al. 1980), and the Limburg Soil Erosion Model (LISEM) (De Roo et al. 1994). Reviews of the existing models have been reported in previous studies (Andualem et al. 2023; Borelli et al. 2021). Sediment transport capacity (TC) is a key component for describing the potential of water flow to transport detached materials. However, interpretations of the TC concept may vary. In models like WEPP and EUROSEM, detachment is constrained by the TC and the current sediment load. According to Wainwright et al. (2015), this approach lacks justification and may be unsuitable. Alternative approaches, such as the Meyer-Peter-Müller (MPM) approach (Meyer-Peter and Müller 1948), represent the actual bedload transport rate (Wainwright et al. 2015). Furthermore, contrasting perspectives regarding the use of capacity (equilibrium) and non-capacity (non-equilibrium) approaches exist (Biswas et al. 2021; Hu et al. 2025). However, since this study focused on bedload, a capacity-based approach was adopted. Different TC approaches have been applied into existing erosion models. Empirical approaches developed from stream data, such as MPM, Ackers-White (Ackers and White 1973), Engelund-Hansen (Engelund and Hansen 1967), and Yalin (Yalin 1963), are widely used in the context of rivers. Although these were developed for stream erosion conditions with low slopes and water depths of several decimeters, some models have applied them to soil erosion. For example, WEPP uses a simplified Yalin approach to calculate TC. In contrast, EUROSEM uses the Govers (1990) approach, which is based on experimental data on overland flow conditions, with steep slopes up to 21%, and shallow water depths.

Because the accuracy of erosion simulations depends on the hydraulic simulation precision, proper consideration and calibration of hydraulics are essential (Morgan et al. 1998b; Smith et al. 1999). However, existing soil erosion models continue to use simplified hydraulic approaches to calculate water forces acting on the soil (Huang et al. 2022).

In addition to erosion models, hydraulic models have also been used to simulate floods and flash floods (Al-Fugara et al. 2023; Hu and Song 2018; Huang et al. 2015; Liang et al. 2016). These vary in accuracy and detail. For example, HEC-RAS (U.S. Army Corps of Engineers, CA, USA) employ a one-dimensional (1D) energy equation, whereas HydroAS (Hydrotec, Aachen, Germany) solves complete shallow water equations, including turbulence and acceleration terms. As the level of accuracy affects computational efficiency, previous studies have explored the acceleration of two-dimensional (2D) models using the LTS

method or GPU acceleration (Hu et al. 2019; Wu et al. 2023). Other studies have focused on the combined modeling of 2D hydraulics and sediment transport during floods. Huang et al. (2022) investigated the impact of sediment on the simulated peak discharge. Existing hydraulic models, such as HydroAS GS/ST (Hydrotec 2025b) and Iber+ (Costabile et al. 2024; García-Feal et al. 2018), support river erosion modeling in combination with hydraulic simulations. Past research has mainly focused on sediment in fluvial flows. Studies on the combination of 2D hydraulics and soil erosion caused by pluvial flows remain scarce. Jia et al. (2023) demonstrated the advantage of a 2D hydraulic approach for simulating soil erosion by comparing observed and simulated data. However, they did not compare these results with existing models that considered simplified hydraulics.

This study focuses on arable land erosion and flash floods that occur as overland flows, unified in one model. In existing soil erosion models, simplified hydraulics are considered, which underestimate rill erosion (Hinsberger 2024).

The core hypothesis is that a detailed hydraulic approach—through a 2D hydrodynamic numerical model that solves complete shallow-water equations—is essential for soil erosion modeling. Such models are currently state-of-the-art for flash flood simulations in Germany. This study aims to simulate soil erosion from a single heavy precipitation event. This was achieved by using a 2D approach, which dynamically updated the topography of the model according to progressive erosion and sedimentation. The TC approach of Govers (1990) was implemented for the required conditions and evaluated using laboratory and plot experiments under heavy precipitation framework conditions. The experiments were chosen to be partially outside Govers' validity range, in order to investigate their influence and provide insight into the applicability and limitations of this approach. Accordingly, a suitable approach for simulating the soil erosion caused by heavy precipitation should be identified. To calibrate the field-scale event data, a sensitivity analysis was performed on different parameters and one influential parameter was selected. Observed natural erosion data from the literature were compared with the simulated results of the combined approach, and existing models demonstrated the improved performance of the combined 2D hydraulic and erosion model. Using a soil erosion model with advanced hydraulics, rill erosion can be accurately simulated in terms of quantitative variation and spatial distribution. Comparing the simulation results of the model used in this study with those of existing models that use simplified hydraulics, demonstrates the benefits of utilizing 2D hydraulics, particularly in the generation of rills. Knowledge of these rills, which contribute significantly to soil erosion, is valuable for erosion management.

2 Materials and Methods

In this study, a combination of a soil erosion approach and a 2D hydrodynamic numerical model was used. The HydroAS model, which is suitable for 2D hydraulic simulations, was selected to represent hydraulic processes (Sect. 2.1). The Govers approach was selected and confirmed as the TC approach to represent soil erosion because of its suitability for overland flow conditions (Sect. 2.2). This approach was implemented within the HydroAS model and applied to experimental plots and field data from the literature (Sect. 2.3 and 2.4).

2.1 Selection of 2D Model

The 2D HydroAS model, which is widely used in Germany for flood and flash flood simulations, was selected for this study (Huber et al. 2021; Lavoie and Mahdi 2017; Yorük and Sacher 2014). To simulate surface runoff, HydroAS solves the complete shallow-water equations and includes the acceleration term, thereby meeting the requirements of this study for accurately simulating erosion driven by overland flow and flash floods. The model can simulate both discharge and rain-on-grid conditions. Infiltration can be considered through sink terms at each mesh node. In this study, heavy precipitation events occurring in early summer were simulated, under the assumption that the soil was dry, water-repellent, and silted due to splash erosion (see Sect. 2.4). As a result, soil processes are negligible, effective precipitation is used as an input parameter for the simulations, and infiltration is excluded. The runoff simulation (both overland and channel flows) was based on Eqs. (1)–(5). Approaches to the roughness, viscosity, and other details can be found in the HydroAS Model Manual (Hydrotec 2025a).

$$\frac{\partial \mathbf{w}}{\partial t} + \frac{\partial \mathbf{f}}{\partial x} + \frac{\partial \mathbf{g}}{\partial y} + \mathbf{s} = 0 \tag{1}$$

with

$$\mathbf{w} = \begin{bmatrix} H \\ uh \\ \mathrm{v}h \end{bmatrix} \tag{2}$$

$$\mathbf{f} = \begin{bmatrix} uh \\ u^2h + 0.5gh^2 - \nu\, h\frac{\partial u}{\partial x} \\ uvh - \nu\, h\frac{\partial \mathrm{v}}{\partial x} \end{bmatrix} \tag{3}$$

$$\mathbf{g} = \begin{bmatrix} \mathrm{v}h \\ uvh - \nu\, h\frac{\partial u}{\partial y} \\ \mathrm{v}^2h + 0.5gh^2 - \nu\, h\frac{\partial \mathrm{v}}{\partial y} \end{bmatrix} \tag{4}$$

$$\mathbf{s} = \begin{bmatrix} 0 \\ gh\,(I_{Rx} - I_{Sx}) \\ gh\,(I_{Ry} - I_{Sy}) \end{bmatrix} \tag{5}$$

where t is the time [s], and x and y represent the streamwise and transverse directions [m], respectively. H is the water level above a reference level [m]; h is the water depth [m]; u and v are components of the flow velocity in x and y directions [m s^{-1}], respectively; g is gravitational acceleration [m s^{-2}]; and Greek letter nu (ν) is the viscosity. The source term $\mathbf{s}$ contains the friction slope I_R and bed slope I_S.

2.2 Governing Erosion Equations

As noted in the Introduction, the HydroAS model can simulate river erosion using its add-on module, GS, which simulates the total sediment load. At each mesh node, the model calcu-

lates the driving forces acting on the soil based on hydraulic parameters. Depending on the selected sediment transport equation, such as MPM or Ackers-White, the TC represents the actual transport rate, and sediment is transported to the following mesh node, where the calculation is repeated. In the existing program, it is possible to specify different particle sizes to consider the layer management. This study used the median grain diameter as a uniform particle size. Soil exchange with the surface (detachment or sedimentation), which leads to changes in topography, was calculated using the Exner equation (Hydrotec 2025b):

$$(1 - n_p)\ \rho_s \frac{\partial Z}{\partial t} + S = 0 \tag{6}$$

where n_p is the porosity of the sediment, ρ_s is sediment density [kg m^{-3}], Z the bed elevation [m], t is the time [s], and S is the balance of sedimentation and erosion [kg m^{-2} s^{-1}]. The soil mass S_e for erosion was calculated as the product of the sink velocity w_s [m s^{-1}], the TC approach, and sediment density ρ_s [kg m^{-3}]:

$$S_e = w_s\, TC\, \rho_s \tag{7}$$

Mass conservation was maintained, as soil mass S was redistributed only among neighboring mesh nodes. However, soil masses can either increase or decrease at the model boundaries. To represent TC, the MPM, Ackers-White, and Engelund-Hansen approaches are pre-integrated into HydroAS GS as the bedload transport rate. In this study, the Govers approach was implemented and is defined as:

$$TC_{Govers} = c * (\omega - \omega_{crit})^d \tag{8}$$

where c and d are parameters dependent on grain diameter. The unit stream power ω [kg m² s^{-3}] is the mathematical product of the slope and the mean flow velocity. The critical unit stream power has a threshold value of 0.004 m/s (Govers 1990). Here, TC_{Govers} also serves as the bedload transport rate. The combined simulation using HydroAS and the Govers approach is referred to as *HydroAS GS–Govers*. In the HydroAS GS–Govers model, no distinction was made between rill and interrill erosion. Rill formation was driven purely by hydraulics.

Initially, the MPM, Ackers-White, and Engelund-Hansen approaches were evaluated for their suitability for soil erosion modeling and compared to the Govers approach (Sect. 3.1).

2.3 Application of the HydroAS GS–Govers Model on Experimental Plots

To evaluate the HydroAS GS–Govers model for soil erosion under heavy precipitation, experimental data were used to compare simulation results with measured observations. These experiments provided clear and traceable boundary conditions and were used as the first validation of the model. The framework conditions of the experimental data were assumed to represent rainfall as heavy precipitation (≥ 15 mm/h according to DWD n.d.) and slope gradients that fit the overland flow conditions. Therefore, a minimum gradient of 5% was determined. Three experimental studies were selected: Quan et al. (2020), Scherer et al. (2012), and Kilinc and Richardson (1973).

Kilinc and Richardson (1973) conducted flume experiments with various slope gradients, rainfall intensities, and one soil type (Table 1). Six runs were selected for this study and named according to their original identifiers (Kil I-IV, Kil IX and Kil X). The 2D model was constructed as a rectangular mesh with 12 elements across the flume width and an aspect ratio of 1:2, following Hydrotec (2025c) guidelines, which suggests a ratio of 1:2 to 1:3. The model was calibrated using runoff and flow velocity values reported by Kilinc and Richardson (1973), with adjustments for surface roughness and rainfall intensity.

Quan et al. (2020) conducted laboratory rainfall experiments on two soils (*AS* from the Ansai Agricultural Experiment Station, and *SD* from the Suide Soil and Water Conservation Experiment Station), with a rainfall intensity of 60 mm/h over one hour and flume gradients of 5°, 10°, 15°, and 20° (Table 1). Although gradients of 15° and 20° exceeded the validity range of the Govers approach (slope < 0.21; see Section 3.1), simulations were still performed. To simulate these experiments, a 2D model was built containing eight elements across the flume width, with an aspect ratio of 1:2. Simulations were named according to soil type and gradient (AS5°–AS20°, SD5°–SD20°). Quan et al. (2020) provided the grain size distribution used to derive d_{50} and measured the total runoff. However, no discharge or flow velocity was provided. Therefore, the amount of rainfall in the simulation was adjusted using a discharge coefficient to determine the indicated total runoff. These coefficients ranged from 0.18 to 0.32, and were used to calibrate the models. The roughness coefficient was not reported in the study; therefore, Manning's n was assumed to be 0.033, based on values stated by Kilinc and Richardson (1973), Scherer et al. (2012), and other studies (e.g., LUBW 2020).

Scherer et al. (2012) reported the field studies conducted in various loess soil areas in Germany by Gerlinger (1997), with 58 experiments on rainfall amount, intensity, and slope. Six experiments were selected (Table 1) to reflect heavy precipitation and erosion conditions in early summer with bare soil, with rainfall intensities of 50.4–64.8 mm/h over 68–75 min, and slopes of 14.7–17.8%. The experiments were grouped into three pairs of plots, and each pair was used to examine the reproducibility and variability of similarly spaced plots (Gerlinger 1997). The 2D model contained eight elements across the flume width, with an aspect ratio of 1:3. The simulations were named according to their original

Table 1 Experimental conditions/information and data input/parametrization for the 2D model of plot models

	Kilinc and Richardson (1973)	Quan et al. (2020)	Scherer et al. (2012)
Name	Kil I-IV, IX, X	AS5°–AS20° SD5°–SD20°	S33–34 S36-37 S40-41
Plot: L × W [m]	4.88 × 1.52	5 × 1	12 × 2
Slope [%]	5.7 15	8.75–36.4	14.7–17.8
Rainfall intensity [mm/h]	31.75–116.84	60	50.4–64.8
Rainfall duration [min]	60	60	68–75
Simulation duration [min]	70	70	120
Simulation time interval [min]	1	1	1
Roughness coefficient (Mannings's n)	0.033	0.033*	0.02–0.04
Median grain diameter (d50)	0.35	0.04–0.044	0.0216–0.0245**
Bulk density [kg/m³]	1500	1300–1350	1670*

* Values are assumptions; **Values derived by Gerlinger (1997)

experimental numbers (S33–34: pair 1; S36–37: pair 2; S40–S41: pair 3). Despite rainfall data, no flow data was available. Therefore, the rainfall was not reduced by any factor in the simulation. Calibration was not performed for the hydraulics. Roughness coefficients used were reported by Scherer et al. (2012). The d_{50} value was derived from the grain-size distribution provided by Gerlinger (1997).

All experimental data were sourced from the literature. Missing values were plausibly estimated. All the values used are presented in Table 1.

All flumes or plots described were designed as 2D models based on the framework conditions outlined in the literature and were simulated using the HydroAS GS–Govers model. In all simulations, the median diameter (d_{50}) was the only fraction used to calculate TC_{Govers}. The simulated sediment transport rates at the flume outlets were compared with the values observed from the literature.

2.4 Application of the HydroAS GS–Govers Model for Field Scale Event Data

Owing to the limitations of laboratory and small-scale field experiments in capturing the full extent of rill erosion, further evaluation of the model was conducted. The model was applied to natural erosion events that occurred in croplands following heavy precipitation.

For this application, three fields presented by Hinsberger (2024) were selected: Fields #4, #7, and #8, where natural erosion was detected and analyzed. These fields were selected because Hinsberger (2024) provided rill erosion estimations and simulation results using the RUSLE2 (Revised USLE 2) and EROSION-3D soil erosion models, which were discussed in this study. The data from Hinsberger (2024) included: (i) orthophotos for the comparison of rill distribution, (ii) measured erosion quantities from rills, (iii) RUSLE2 total erosion, and (iv) EROSION-3D simulation results. The results of the RUSLE2 and EROSION-3D (E3D) models used in this study are presented in Table 2.

For the simulation, precipitation rates were derived from YW radar data provided by the German Meteorological Service (Deutscher Wetterdienst DWD). As Hinsberger (2024) did not specify any effective precipitation or discharge data, the total precipitation was assumed for the simulations. In Europe, this neglect of infiltration is partially justified, as heavy precipitation often occurs in early summer, when soils are dried out and silted. As recorded rill erosion occurred in June (Hinsberger 2024), these assumptions were supported.

Digital elevation models (DEM) provided by Hinsberger (2024) served as the simulation basis. Pre-erosion DEMs with centimeter-level resolutions were resampled to grid sizes of

Table 2 Results of measurements, RUSLE2 and EROSION-3D (E3D) models from Hinsberger (2024) used in this study. When no results were provided, - is shown in the table

	Total erosion [t/ha]		Rill erosion [t]		
	RUSLE2	E3D	measured	RUSLE2	E3D
#4	13.14	0.30			
Rill #4.1			11.75	1.14	0.02
Rill #4.2			8.03	1.32	-
#7	65.15	10.45			
Rill #7.6			17.39	11.71	1.35
Rill #7.7			14.67	6.93	-
Rill #7.8			13.28	7.81	0.57
Rill #7.10			5.71	5.76	-
#8	12.32	4.84			
Rill #8			15.79	6.11	4.34

0.25 m (DEM0.25) and 1 m (DEM1). Therefore, the model was built as a mesh using square elements of 0.25 × 0.25 m and 1 × 1 m.

Different calibration parameters for the models are possible, including surface roughness, grain diameter, and a factor for the transport capacity ($k \times TC_{Govers}$). A sensitivity analysis of the surface roughness parameter (Manning's n) and median grain diameter (d_{50}) was conducted. Manning's n was selected as a parameter to examine the influence on runoff, as it is state-of-the-art in flood modeling (e.g., Ferguson 2021). Grain size was selected because it is the only input parameter in the Govers equation suitable for sensitivity analysis. Both parameters were reduced and increased for each simulation. Manning's n was adjusted to a plausible range for the surface roughness for croplands (Aigner and Bollrich 2015; Chow 1959). Although studies have indicated that Manning's n is higher for overland flow (Sanz-Ramos et al. 2021) and that water depth depends on shallow-water flow (Hinsberger et al. 2022), this sensitivity analysis was reduced to the essential influence of roughness. Grain diameter was adjusted in a range of ± 30–40%. As a change in the grain diameter leads to a change in the surface roughness, this relationship was disregarded. Simulations were conducted using the original TC_{Govers} (Eq. 8). As TC_{Govers} is the most uncertain calibration parameter, the models were calibrated to the measured rill quantities from the literature using a factor named 'Cali' (Table 3). Calibration was conducted for DEM1, which was more commonly available.

Table 3 presents an overview of the simulations and corresponding framework conditions. The simulation names consist of the DEM basis (1 m or 0.25 m grid) and the adapted parameter for the sensitivity analysis. The experiments were conducted in Fields #4, #7, and #8. Experiments Exp. DEM1 and Exp. DEM1 (Cali) were used for comparison with the measured data and results from RUSLE2 and E3D. Other simulations were used for sensitivity analysis. Table 4 presents basic information on field and event data and hydrodynamic model parameterization.

Table 3 Overview of simulations and sensitivity parameters for the fields #4, #7, and #8

Experiment	Manning's n [$s/m^{1/3}$]			Median grain diameter d_{50} [mm]		
	#4	#7	#8	#4	#7	#8
Exp. DEM1	0.033	0.033	0.033	0.060	0.050	0.306
Exp. DEM1 (Cali)	0.033	0.033	0.033	0.060	0.050	0.306
Exp. DEM 0.25	0.033	0.033	0.033	0.060	0.050	0.306
Exp. DEM 1 n reduced	0.025	0.025	0.025	0.060	0.050	0.306
Exp. DEM 1 n increased	0.050	0.050	0.050	0.060	0.050	0.306
Exp. DEM 0.25 n reduced	0.025	0.025	0.025	0.060	0.050	0.306
Exp. DEM 0.25 n increased	0.050	0.050	0.050	0.060	0.050	0.306
Exp. DEM 1 d reduced	0.033	0.033	0.033	0.040	0.030	0.200
Exp. DEM 1 d increased	0.033	0.033	0.033	0.080	0.070	0.400
Exp. DEM 0.25 d reduced	0.033	0.033	0.033	0.040	0.030	0.200
Exp. DEM 0.25 d increased	0.033	0.033	0.033	0.080	0.070	0.400

Table 4 Experimental conditions/information and data input/parametrization for the 2D model of field-scale models

Name	#4	#7	#8
Field extension [hectare]	1.10	6.61	4.37
Max. Rainfall intensity [mm/h]	20.35	48.23	33.01
Rainfall duration [min]	55	90	90
Simulation duration [min]	120	120	120
Time interval [min]	5	5	5
Roughness coefficient (Mannings's n)	0.033	0.033	0.033
Median grain diameter (d50)	0.060	0.053	0.306
Bulk density [kg/m³]	1120	1420	1300

In many models, such as WEPP and EUROSEM, the erosion calculation is separated into interrill and rill shares or raindrop-induced and overland flow erosion (as in E3D). As the contribution of splash erosion is less impactful than that of the rill share (Govers and Poesen 1988), the splash erosion share was neglected.

The simulation results, including a modified topography (see Sect. 2.2), can be converted into a DEM with the same resolution as the input of the simulation. The difference between the original surface height (DEM0.25 or DEM1) and surface height at the final time step produces the erosion depth at each grid point, which can be converted to erosion quantities using bulk density. In addition, predefined cross sections provide information on the sediment load for each time step.

3 Results and Discussion

This study employed the Govers approach as the TC approach for soil erosion modeling, in combination with the 2D HydroAS model. The model was applied to experimental plots and real-world field conditions. Section 3.1 evaluates the suitability of this approach by examining the validity ranges of different TC approaches. The simulation results of the HydroAS GS–Govers model for experimental flumes/plots and naturally occurring erosion are presented and analyzed in Sect. 3.2 and 3.3, respectively.

3.1 Suitability of Govers (1990) Approach for Soil Erosion Modeling

Various TC approaches are available for erosion modeling. However, these approaches have been empirically calibrated from experiments using specific setups and soil properties. Therefore, each approach is only applicable to experiments within the specific validity range for which it was developed (Brazier et al. 2011). Figure 1 compares the validity ranges of the MPM, Ackers-White, Engelund-Hansen, and Govers TC approaches for the grain diameter and slope parameters. The MPM, Ackers-White, and Engelund-Hansen approaches have already been implemented into HydroAS GS, and the Govers approach is a part of the well-known EUROSEM (Morgan et al. 1998a) and LISEM (De Roo et al. 1994) models. The ranges for MPM, Ackers-White, and Engelund-Hansen were obtained from a compilation by BMLFUW and ÖWAV (2011), and the range for Govers was derived from Govers (1990). Notably, the slope parameter indicates different conditions: MPM, Ackers-White, and Engelund-Hansen showed validity for small slopes (<4%) indicating river conditions and a wide range of grain diameters. In contrast, Govers exhibited validity

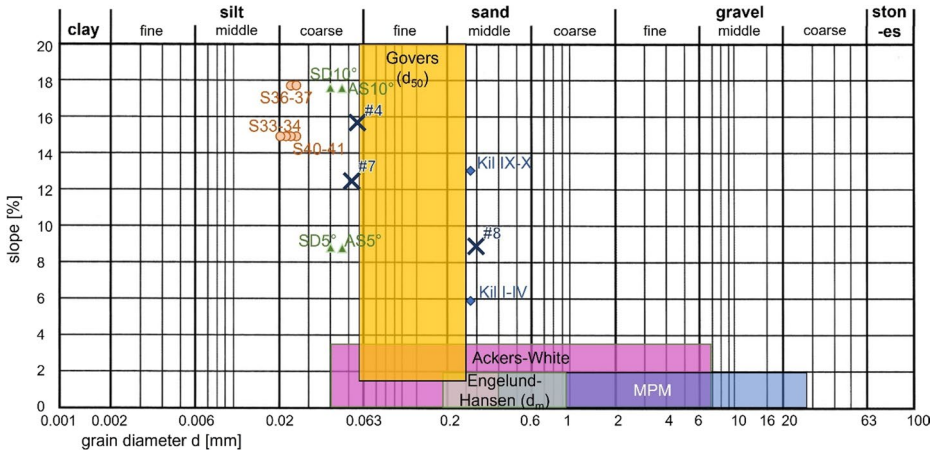

Fig. 1 Validity range of different transport capacity approaches. For the grain diameter, the range of experimental sediments used are shown for Ackers-White and MPM, the range of the mean diameter (d_m) for Engelund-Hansen, and the range of the median diameter (d_{50}) for Govers. The x symbols, dots, triangles, and diamonds indicate the median grain size d_{50} and mean slope of investigations by Hinsberger (2024), Scherer et al. (2012), Quan et al. (2020), and Kilinc and Richardson (1973), respectively. Each symbol represents an erosion field or an experimental run

for a wide range of slopes (<21%), including overland flow conditions, and a more limited range of grain diameters.

In addition, Fig. 1 shows the grain diameter and slope characteristics for the experimental plots and fields with naturally occurring erosion due to heavy precipitation. Due to the inclusion of the experiments used for the evaluation in this study, the validity range of Govers is significantly more appropriate than that of the comparative approaches. All experiments fall within Govers' validity range for slope. Regarding the grain diameter, the selected experiments were conducted outside Govers' approach. However, the experimental soil properties were similar to those used in the study by Govers (1990). In addition to the slope and grain diameter, the boundary conditions for erosion due to heavy precipitation events were of primary importance when selecting the experiments (see Sect. 2.3). This perception and selection of the approach agree with those of Wang et al. (2019), who stated that the Govers approach was the best for cropland soil.

3.2 Evaluation of the HydroAS GS–Govers Model for Experimental Plots

Data from Kilinc and Richardson (1973), Scherer et al. (2012), and Quan et al. (2020) were used to simulate rainfall in the experimental plots, using the HydroAS GS–Govers model. The framework conditions (median grain diameter and slope) are illustrated in Fig. 1. The experiments conducted by Kilinc and Richardson, Scherer et al., and Quan et al. are highlighted by blue diamonds, orange dots, and green triangles, respectively. The figure indicates that the slope values fall within the validity range of the Govers approach. However, the median grain diameter d_{50} of the soil used by Kilinc and Richardson was coarser than that used by Govers, whereas the soils used by Scherer et al. and Quan et al. had finer median grain diameters.

The simulated results were compared with measurements from the literature to evaluate model suitability. To ensure comparability, as Scherer et al. (2012) and Quan et al. (2020) merely reported total detachment, the results of this study were adjusted by considering the total sediment that reached the outlet of the model during the simulation. The same procedure was followed for the results presented by Kilinc and Richardson. The observed data from the literature and the results of the HydroAS GS–Govers model are listed in Table 5.

The simulated results were compared with the measured data. Figure 2 compares the cumulative measured erosion (x-axis) with the cumulative simulated erosion (y-axis) for each experiment. Different erosion quantity ranges were included in the experiments.

The simulation results for the experiments by Kilinc and Richardson indicated extremely low erosion rates. Experiments with low precipitation and discharge (Kil I and II) showed no erosion. Higher precipitation rates or steeper slopes (Kil III, IV, IX, and X) resulted in minimal erosion, with values approaching zero. This suggests that the threshold value for the critical unit stream power in the approach (0.004 m/s; see Eq. 8), which is an empirically derived constant, was too high for these experimental conditions. As shown in Fig. 1, the d_{50} values of the Kilinc and Richardson experiments were coarser than those of the Govers approach. Therefore, the threshold value must be adjusted to produce greater erosion in those conditions. Accordingly, the statistical values for the suitability of the model showed high deviation (Table 6).

In the experiments of Quan et al., the observed and simulated values showed high agreement (Fig. 2). Differences related to soil type (AS, orange; SD, green) were notable. The simulation results for SD soils (green triangles) were in high agreement with measured data, with an RMSE of 0.20. Notably, the experiment SD of 5° with the lowest erosion quantity

Table 5 Total detachment [kg] presented or derived from the literature (Quan et al. 2020; Scherer et al. 2012; Kilinc and Richardson 1973) and HydroAS GS–Govers simulation results of experimental flumes/plots

Experiment	Results from the literature	HydroAS GS-Govers
Quan et al. (2020)		
AS 5°	0.143	0
AS 10°	0.834	0.540
AS 15°	0.994	0.666
AS 20°	1.375	0.665
SD 5°	0.021	0.095
SD 10°	0.207	0.207
SD 15°	0.373	0.389
SD 20°	0.549	0.901
Kilinc and Richardson (1973)		
Kil I	0.776	0
Kil II	2.425	0
Kil III	5.222	0.014
Kil IV	11.980	0.029
Kil IX	5.129	0.029
Kil X	27.833	0.115
Scherer et al. (2012)		
S33	9.6	29.604
S34	14.7	35.171
S36	57.9	37.138
S37	22.9	39.543
S40	47.7	23.941
S41	31.0	32.996

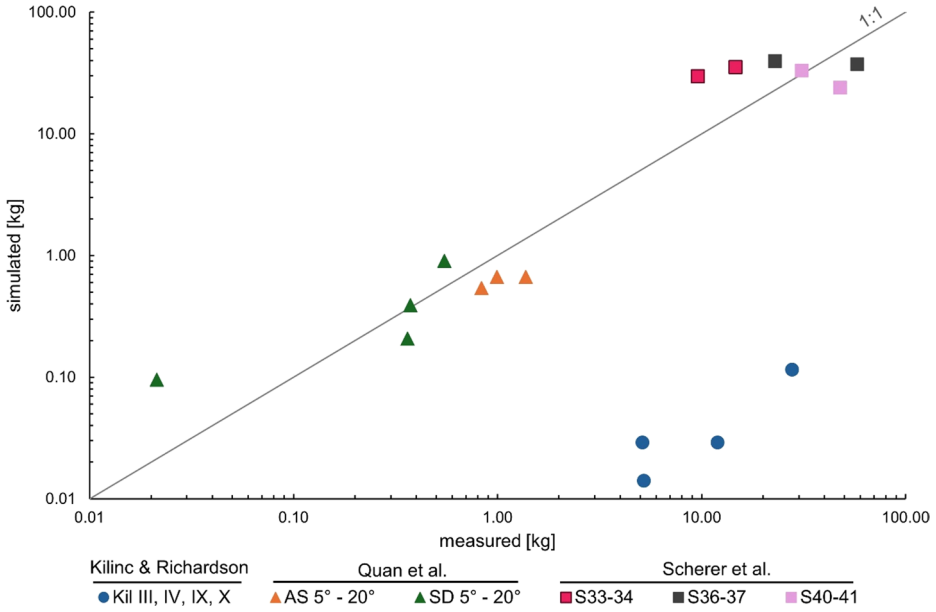

Fig. 2 Comparison of simulated erosion [kg] using the 2D HydroAS GS–Govers model (ordinate) with respective measured erosion data from Kilinc and Richardson (1973) (blue dots), Quan et al. (2020) (orange and green triangles) and Scherer et al. (2012) (pink, grey and rose squares)

showed strong agreement at the onset of sediment transport. In contrast, the AS simulations (orange triangles) consistently underestimated erosion measurements (RMSE = 0.42). Experiments SD 15° and 20° and AS 15° and 20° exhibited the highest erosion and fell outside the validity range of the Govers approach (see Sect. 2.3). The SD simulations overestimated erosion, while AS simulations underestimated it. Despite the limited number of simulations, these results suggest that the Govers approach can be applied to higher gradients than those shown in the validity range in Fig. 1. Overall, the HydroAS GS–Govers results fit the measured erosion with an RMSE of 0.33, indicating good agreement.

Figure 2 also presents simulated and observed data from Scherer et al. (squares). Different colors indicate different experimental pairs, representing the reproducibility and variability of the adjacent plots. Pairs sometimes showed significant divergence. For S33–S34, the simulation matched the trend for both experiments: an overestimation of erosion. For S36–S37 and S40–S41, the simulated erosion for the pairs was similar; however, the mea-

Table 6 Statistics for the difference between the experimental results and the results of the HydroAS GS–Govers model. mean = mean value, mae = mean absolute error, rmse = root mean square error (all values in kg)

	Kilinc and Richardson – HydroAS GS–Govers	Quan et al. – HydroAS GS–Govers	Scherer et al. – HydroAS GS–Govers
Mean	8.86	0.15	−2.43
MAE	8.86	0.26	17.27
RMSE	12.72	0.33	18.69

surements varied significantly. This suggests that although the scatter in the measured data is quite high, the simulation results indicate a plausible value, as one experiment overestimates and the other underestimates. These experiments fall within the slope validity range of the Govers approach but show smaller values for the grain diameter. However, the simulated results using HydroAS GS–Govers and the observed values showed good agreement (Table 6), suggesting the lower deviation of the grain diameter had limited influence on suitability.

In summary, the comparison between the validity range and the simulation of the laboratory and plot experiments showed that the Govers approach is suitable for simulating soil erosion caused by heavy precipitation. However, exceeding the valid grain diameter range (as in Kilinc and Richardson) had a strong influence on the erosion quantity, and the HydroAS GS–Govers model significantly underestimated the erosion. Interestingly, a smaller grain diameter than suggested influences the suitability of Govers' approach less (as in Scherer et al.). Therefore, exceeding the maximum grain diameter beyond the validity range should be avoided. Possibly, another TC approach for larger grain diameter could address this limitation. Exceeding the validity range of the slope (as in Quan et al.) did not adversely affect the simulation results.

As small plots do not represent the total influence of the catchment area (Brazier et al. 2011), and the relevance of the two-dimensional hydrodynamic numerical hydrologic approach may be limited under simple framework conditions, the HydroAS GS–Govers model was further tested on natural erosion fields.

The following section focuses on erosion at the field-scale based on measured data and simulation results from other soil erosion models.

3.3 Evaluation of the HydroAS GS–Govers Model for Naturally Occurring Erosion

To simulate erosion at the field scale using the HydroAS GS–Govers model, fields #4, #7, and #8 were investigated and analyzed by Hinsberger (2024). The framework conditions (median grain diameter and slope) for these fields are shown in Fig. 1 and highlighted by black crosses. Slope conditions lie within the validity range of the Govers approach, whereas the grain diameter is finer for fields #4 and #7 and coarser for field #8.

For naturally occurring erosion at the field scale, a sensitivity analysis for Manning's n and the median grain diameter was first conducted (Sect. 3.3.1). Then, the total erosion rates, rill erosion quantities, and spatial distribution of the rills were compared with the measured data and results from the RUSLE2 and E3D models (Sect. 3.3.2 and 3.3.3).

3.3.1 Sensitivity Analysis and Calibration

A sensitivity analysis was conducted to assess the influence of selected input and possible calibration parameters.

Morgan et al. (1998b) stated that erosion depends heavily on hydraulic considerations. However, no hydrological measurements were available from Hinsberger (2024); therefore, the hydraulics could not be calibrated. Hence, surface roughness was selected as the sensitivity parameter because of its influence on flow velocity and, consequently, TC_{Govers}. Median grain diameter (d_{50}), the only soil parameter influencing TC_{Govers} (Eq. 8), was selected as the second sensitivity parameter. The sensitivity analysis was conducted using DEMs with

grid resolutions of 1 m and 0.25 m to investigate the influence of grid size. A summary of the simulations and their modifications is presented in Table 3.

The results of the sensitivity analysis are shown in Fig. 3. The simulated erosion was set in relation to the measured value. A value of one (y-axis) represents perfect agreement, a value > 1 represents overestimation, and a value < 1 indicates underestimation. The figure shows three rills named #7.6, #7.10, and #8 (Fig. 5). Rill #7.10 (green) represents a small rill, and #7.6 (dark yellow) and #8 (blue) represent large rills (Table 2). Triangles and crosses indicate the simulation bases using DEM1 and DEM0.25, respectively.

To analyze the surface roughness, Manning's n was reduced and increased compared with the original assumption. A reduced n indicates a smoother surface and an increased n a rougher surface. As shown in Fig. 3a, a reduced n value resulted in greater erosion, whereas a higher n value resulted in less erosion for both DEM1 and DEM0.25. This trend is plausible because an increased flow velocity occurs with a smoother surface framework, resulting in higher forces acting on the soil. In Fig. 3b, the sensitivity analysis of the median grain diameter d_{50} is shown. A reduction in d_{50} led to an increase in erosion, whereas an increase in d_{50} led to a decrease in erosion. This is again plausible because of the increased transport capacity of smaller soil particles. Contrary to expectations, two key trends emerged: (i) Smaller rills (#7.10 < #7.6, #8) were more sensitive to the influence of changes in roughness or grain diameter, especially for rill #7.10, where the sensitivity to d_{50} was significant with variations of up to +61% (reduced diameter) and -25% (increased diameter); (ii) Smaller rills were also more affected by grid resolution. Rill #7.10 showed significant differences between the 1 m and 0.25 m grids, ranging from -59% for a reduced d_{50} and -39% for an increased d_{50}. In contrast, for rill #8, the results for the 1 m and 0.25 m grids were almost identical (Table 7), and no clear trend could be derived. This can be attributed to the thalweg of rill #8. The grid resolution is a significant factor in estimating the erosion quantities for rills. In a 1 m grid, the discharge accumulates in one grid cell, while a 0.25 m grid provides four cells on the same grid width. Consequently, small rills were overestimated when a grid size of 1 m was used, whereas a higher grid resolution led to more accurate simulation results. This hypothesis is supported by the results for rill #8, which produced similar erosion quantities at both grid resolutions. However, high model resolutions can lead to a

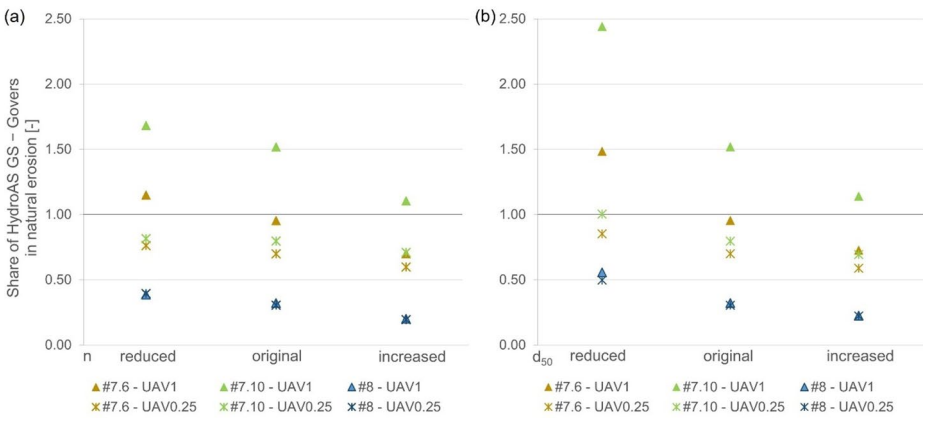

Fig. 3 Sensitivity of Manning's n (**a**) and median grain diameter d50 (**b**) for selected rills based on simulated and measured rill erosion quantities

Table 7 Rill erosion [t] for visible rills using different experimental runs

Experiment	#4.1	#4.2	#7.6	#7.7	#7.8	#7.10	#8
DEM1	2.37	2.00	16.59	10.87	5.24	8.67	5.08
DEM1, Cali	11.25	8.16	19.57	13.17	6.22	10.32	15.42
DEM0.25	2.81	2.11	12.16	8.28	3.87	4.55	4.82
DEM1, n reduced (n = 0.025)	2.87	2.44	19.98	12.69	6.16	9.61	6.09
DEM1, n increased (n = 0.050)	1.74	1.46	12.18	7.17	3.81	6.31	3.18
DEM0.25, n reduced (n = 0.025)	3.23	2.39	13.25	8.63	4.45	4.65	6.23
DEM0.25, n increased (n = 0.050)	2.04	1.56	10.41	6.44	2.89	4.06	3.08
DEM1, d reduced (−30 – −40%)	3.48	2.88	25.81	18.82	8.24	13.94	8.79
DEM1, d increased (+30 – +40%)	1.76	1.49	12.64	7.66	3.99	6.51	3.56
DEM0.25, d reduced (−30 – −40%)	3.68	2.75	14.83	9.50	4.84	5.73	7.86
DEM0.25, d increased (+30 – +40%)	2.15	1.62	10.23	6.80	3.06	3.96	3.51

decrease in computational efficiency. The issue of computational efficiency was investigated by Hu et al. (2019) and Wu et al. (2023), although it was not the primary focus of this study. The findings on the importance of DEM resolution are consistent with the results of Jia et al. (2023) who highlighted the advantages of using both high-resolution topography and numerical simulations.

The HydroAS GS–Govers model showed high sensitivity to both surface roughness and grain diameter. Modeling results were further influenced by grid resolution. Rill quantities derived from DEM0.25 matched the measured quantities more accurately than those derived from DEM1. However, a high-quality DEM with these grid resolutions is not always available for soil erosion modeling. Overall, the HydroAS GS–Govers model simulated less erosion than the observed values.

Therefore, the models were calibrated using a factor for TC_{Govers}. The models were calibrated to the measured rill quantities using this factor (Experiments named 'Cali'). Calibration was conducted for DEM1 because this database is commonly available.

Each field was calibrated to fit observed rill quantities (Exp. DEM 1, Cali). The factors in the TC_{Govers} equation (Eq. 8) depend on the field and are 10, 1.2, and 3 for fields #4, #7, and #8, respectively.

3.3.2 Total Erosion

The total erosion rate is the standard output of RUSLE2, which is part of the USLE family and a well-established method for erosion estimation. For the grid-based simulation models (E3D and HydroAS GS–Govers), elevation changes between the first and final time steps—as well as the bulk density—were used to calculate total field erosion. The simulation results for total erosion are listed in Table 8.

Figure 4 compares the erosion rates simulated using the HydroAS GS–Govers model (Exp. DEM1) with rates from RUSLE2 and E3D (Table 2). Both RUSLE2 and E3D pre-

Table 8 Total erosion [t/ha] for each field using different experimental runs

Experiment	#4	#7	#8
DEM1	22.94	81.43	4.07
DEM1, Cali	201.63	101.33	12.54
DEM0.25	35.22	86.35	6.35

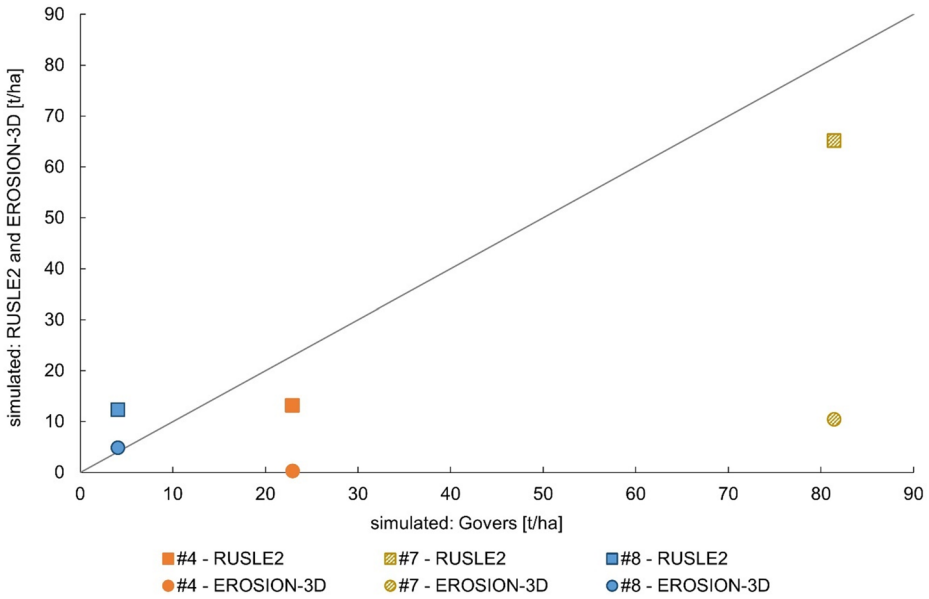

Fig. 4 Comparison of the total erosion rate [t/ha] using the Govers approach (Exp. DEM1) (x-axis) and the RUSLE2 (y-axis, rectangle) or E3D (y-axis, dot) for different croplands (#4, #7, and #8)

dicted higher erosion rates in field #8 and lower erosion rates in fields #4 and #7. E3D, in particular, predicted significantly lower rates than RUSLE2 and HydroAS GS–Govers, whereas RUSLE2 values were only 14–40% lower than HydroAS GS–Govers for fields #4 and #7. Statistical values comparing RUSLE2 and HydroAS GS–Govers results (Table 9) revealed strong agreement. Field #8 may have been influenced by a relatively large d_{50} which exceeded the validity of the Govers approach (see Sect. 3.1), resulting in a TC that was too low to achieve sufficient erosion. In Exp. DEM1 (Cali), the model was calibrated to observed rill values. A comparison of the total erosion of the calibrated and RUSLE2 models shows strong deviations. In Table 9, the statistical values for a comparison of RUSLE2

Table 9 Statistics for the difference between the RUSLE2 and E3D model results and the results of the HydroAS GS–Govers model Exp. DEM1 and Exp. DEM1 (Cali). mean = mean value, mae = mean absolute error, rmse = root mean square error (all values in t/ha)

	RUSLE2 – HydroAS GS–Govers (Exp. DEM1)	RUSLE2 – HydroAS GS–Govers (Exp. DEM1, Cali)	E3D – HydroAS GS–Govers (Exp. DEM1)	E3D – HydroAS GS–Govers (Exp. DEM1, Cali)
Mean	−5.94	−74.96	−30.95	−99.97
MAE	11.44	74.96	31.46	99.97
RMSE	11.96	110.81	43.02	127.61

and E3D with the uncalibrated and calibrated HydroAS-GS–Govers model indicate that the uncalibrated model fits RUSLE2 better. Because it is assumed that RUSLE2 provides plausible results for total erosion, the calibration of the rill quantities overestimates the total erosion.

All simulations were conducted using standard parameter values. While HydroAS GS–Govers and RUSLE2 did not have many calibration parameters, E3D provided several opportunities to calibrate the model results. However, the comparative values were obtained from the literature, and the aim of this study was not to calibrate RUSLE2 or E3D.

In conclusion, the HydroAS GS–Govers and RUSLE2 models produced comparable results, although RUSLE2 was easier to apply and more time efficient. This overall good agreement with RUSLE2 aligns with the observations of Batista (2025), who reported on the prevalence of USLE family models in the literature on soil erosion modeling. However, RUSLE2 only provides an estimate for the entire field and offers no information on the occurrence of rill erosion. In contrast, grid-based models, such as E3D and HydroAS GS–Govers, can simulate accumulated discharge and resulting accumulate erosion. Here, computational efficiency is reduced when using a 2D hydraulic approach compared with the simplified hydraulics used in E3D. However, the focus of this study was to apply and analyze the impact of the 2D model, making the computational cost and efficiency less relevant.

3.3.3 Rill Erosion

In this study, both the HydroAS GS–Govers and E3D models indicated rill erosion. Rills were identified visually using varying symbologies and hillshades, following the method described by Hinsberger (2024). In field #4, E3D simulated one rill, whereas HydroAS GS–Govers simulated two naturally occurring rills (#4.1–4.2). In field #7, the natural event formed ten rills, of which E3D simulated two and HydroAS GS–Govers simulated four (#7.6–7.10). In field #8, both models simulated one rill that occurred in the thalweg during the rainfall event. The rill identifiers were assigned according to the system in Hinsberger (2024), and are shown in Fig. 5.

The spatial distribution of simulated rills matched well with that of the orthophotos in both models. A comparison between the orthophotos and the HydroAS GS–Govers simulation results is presented in Fig. 5. In field #4 (Fig. 5a and b), both rill types–the two large rills (#4.1 and #4.2) and many smaller rills that occurred during the natural event–are visible in the HydroAS GS–Govers simulation. Field #7 (Fig. 5c and d) reproduced many rills that occurred during the event in the simulation. In field #8, one large rill in the thalweg (#8) appeared in both the orthoimage (Fig. 5e) and simulation results (Fig. 5f).

Thus far, the HydroAS GS–Govers model has shown greater accuracy in simulating the spatial distribution of rills. RUSLE2 does not provide any information on rill distribution, and E3D consistently simulated fewer rills than observed. The advantage of simulating rills using a 2D hydraulic model was also demonstrated by Jia et al. (2023). They found that the evolution of the channel network was accurately simulated.

The HydroAS GS–Govers model produced results for water depth, flow velocity, and discharge using the hydraulic approach, and sediment transport using the erosion approach. Figure 6 shows the discharge and sediment load hydrographs at the end of each rill. A comparison of rill erosion quantities in Table 7 with the cumulative sediment load reveals a significant discrepancy. For instance, rill #8 exhibited an erosion quantity of 15.42 tons as

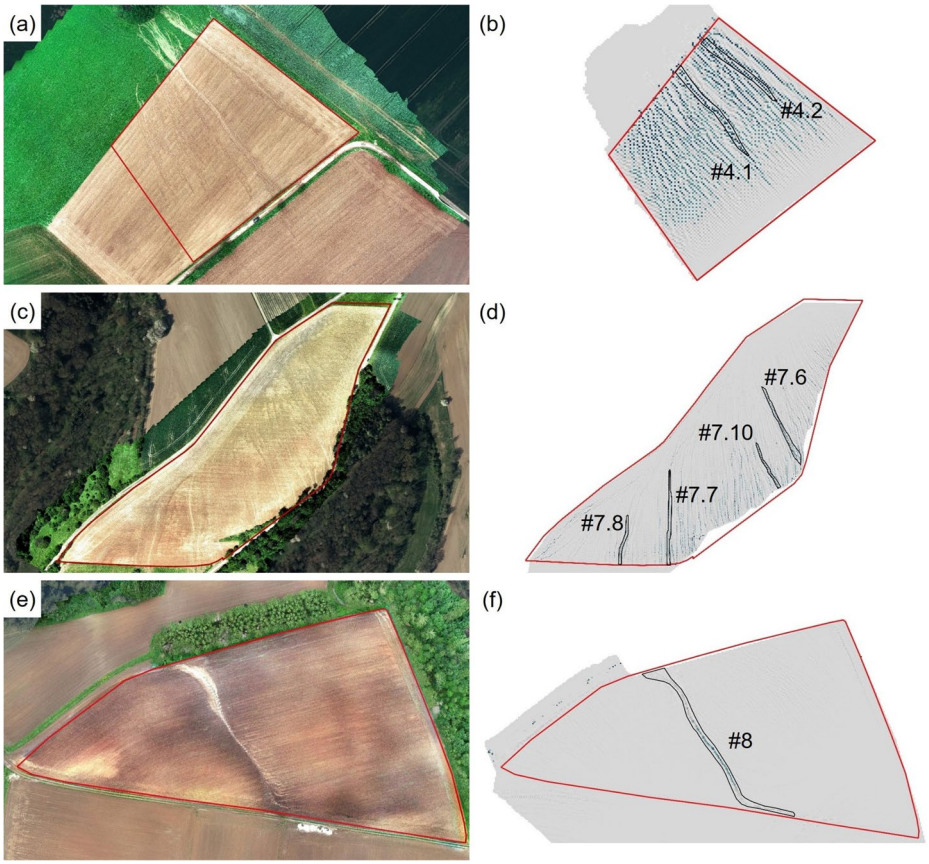

Fig. 5 Orthophotos and simulation results of HydroAS GS–Govers (Exp. DEM1 Cali) shown as elevation changes using hillshades, with changes ≥ 1 cm for fields #4, (**a**) and (**b**); #7, (**c**) and (**d**); and #8, (**e**) and (**f**). The black outline indicates the identified rills and their corresponding names. Orthophotos (a), (c), and (e) are edited for better visibility of the rills

calculated from the erosion depth, whereas the sediment load reaching the end of the flume was only 1.66 tons for Exp. DEM1 (Cali). This indicates that a large portion of the eroded material was deposited in the field and did not reach the end of the rill. However, the simulation results imply that sedimentation mostly occurred in the field, rather than neighboring areas, contrary to the apparent erosion observed in the orthophotos.

In addition to the spatial distribution, the accuracy of rill erosion quantities is an important factor in evaluating model quality. To evaluate the rill erosion quantities, the results of HydroAS GS–Govers, E3D, and RUSLE2 (applied to the rill catchment area) were compared with the measured rill erosion for fields #4, #7, and #8. For the HydroAS GS–Govers model, the uncalibrated (Exp. DEM1) and the model calibrated using observed data (Exp. DEM1 Cali) were analyzed.

Figure 7 shows comparisons between the measured data with the model results of HydroAS GS–Govers Exp. DEM1, Cali (Fig. 7a); Exp. DEM1 (Fig. 7b); RUSLE2 (Fig. 7c); and E3D (Fig. 5d). The uncalibrated HydroAS GS–Govers model (Fig. 7b) tended to under-

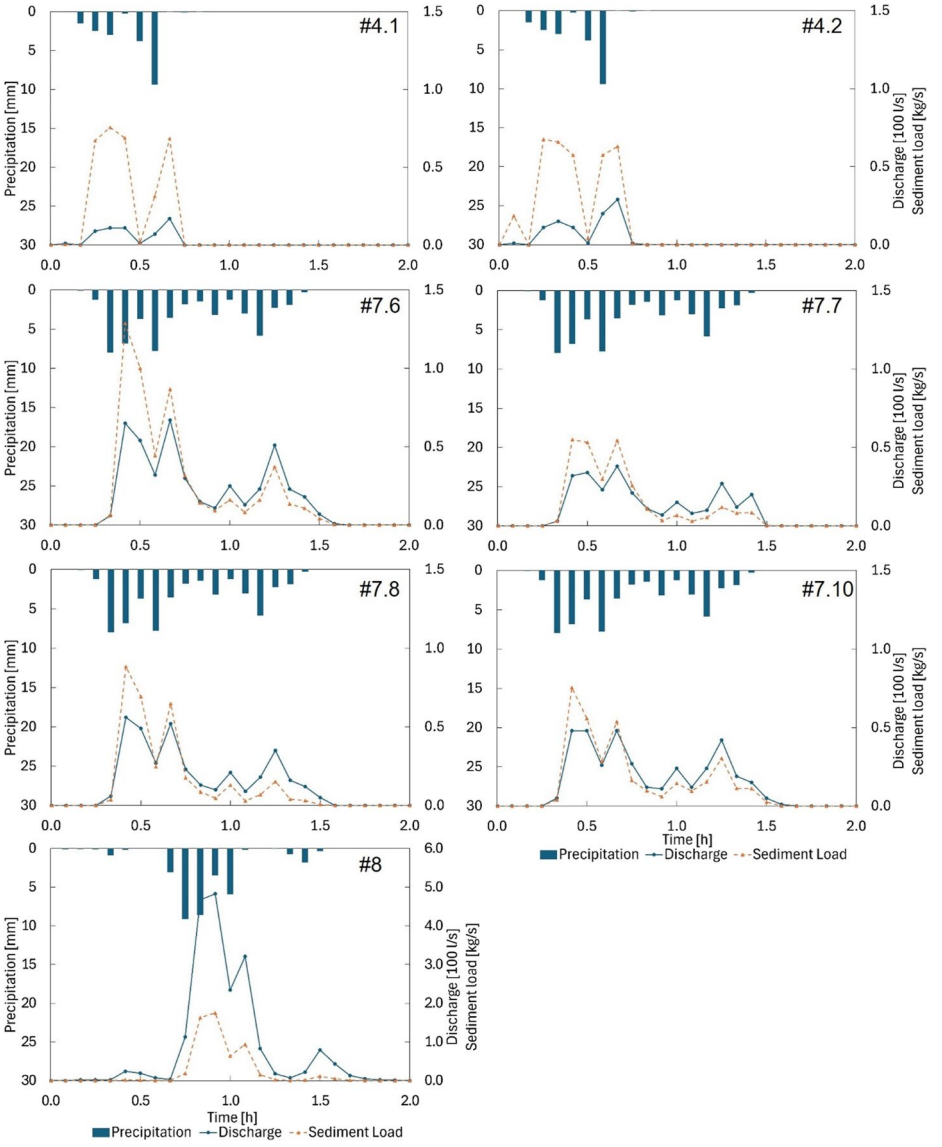

Fig. 6 Results from simulations Exp. DEM1 (Cali): Discharge (blue line) and sediment load (orange, dashed line) hydrographs at the end of the rills and precipitation input of the model (blue bars). Discharge/ Sediment load axis for #8 differs from the others

estimate rill erosion for most rills, particularly in fields #4 and #8, as well as rill #7.8. These rills were larger than others and suffered more erosion. Rill #7.10, which was smaller and less pronounced (Table 2; Fig. 7d), was overestimated using the HydroAS GS–Govers model. Overall, the simulation resulted in a mean difference of −5 tons. The calibrated HydroAS GS–Govers achieved better results with a mean difference of −0.36 tons. RUSLE2 results were comparable, with large rills being overestimated and smaller rills aligning more

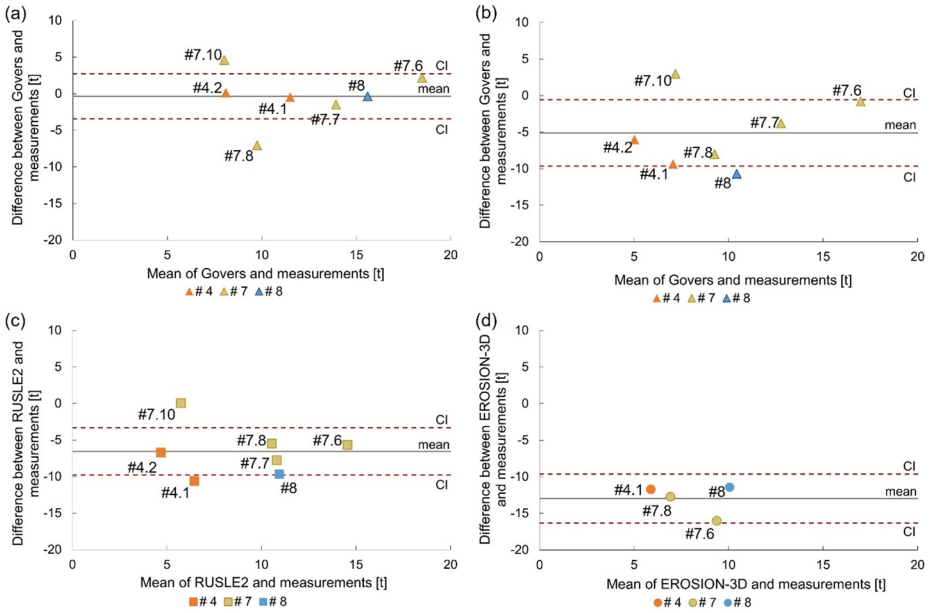

Fig. 7 Bland-Altman plots comparing the calibrated HydroAS GS–Govers model (Exp. DEM1 Cali) (**a**), the uncalibrated HydroAS GS–Govers model (Exp. DEM1) (**b**), RUSLE2 (**c**), and E3D (d). Each data point represents one rill, with different colors representing different fields. The confidence interval (CI) was calculated as the sum of the mean and the quotient of the t distribution (95%, n-1) *standard deviation and the square root of n

closely to the measurements, showing a mean difference of −6.5 tons. In contrast, E3D results indicated an even greater underestimation of the measurements, with a mean difference of −13 tons in erosion. Overall, the statistical values of the observed and simulated erosion quantities (Table 10) show that HydroAS GS–Govers fits the measurements better than other models, particularly when calibrated.

A comparison of the rill erosion quantities of the HydroAS GS–Govers model with those of RUSLE2 and E3D showed that RUSLE2, applied to predefined rill catchments, delivered estimates of the same order of magnitude as HydroAS GS–Govers. In contrast, E3D produced much lower erosion estimates for both the total and rill erosion rates. Given that this study aims to assess the advantages of a 2D hydrodynamic numerical approach, a comparison of grid-based models is particularly relevant. HydroAS GS–Govers offers several

Table 10 Statistics comparing the difference between the observed erosions and the results of the RUSLE2, E3D, and HydroAS GS–Govers model Exp. DEM1 and Exp. DEM1 (Cali). mean = mean value, mae = mean absolute error, rmse = root mean square error, NSE = Nash–Sutcliffe efficiency coefficient. (All values in tons)

	Observed – RUSLE2	Observed – E3D	Observed – HydroAS GS–Govers (Exp. DEM1)	Observed – HydroAS GS–Govers (Exp. DEM1 Cali)
Mean	−6.55	−12.98	5.11	−0.36
MAE	6.56	12.98	5.96	2.34
RMSE	7.30	13.11	6.84	3.35
NSE	0.86	0.77	0.85	0.94

advantages, including the consideration of precise hydraulics and adaptability to complex topography, improving flow and erosion calculations. Its superior ability to simulate rill formation in terms of spatial distribution and erosion quantities holds promise for future soil erosion modeling.

4 Conclusions

This study investigated the Govers approach as a TC approach integrated with the 2D hydrodynamic numerical model HydroAS. Comparisons of the validity ranges for different TC confirmed that the Govers approach is suitable for soil erosion modeling. Using this combined 2D hydraulic and soil erosion model, plot-scale and event-scale data were successfully simulated. Comparisons between observed and simulated erosion plot data demonstrated that the approach is suitable for the entire validity range of the slope and for higher values as well as lower grain diameters than those shown in the validity range. However, the maximum grain diameter used by Govers should not be exceeded.

Simulations of event-based sheet and rill erosion showed substantial improvements over existing models. Regarding the spatial rill distribution, results corresponded well with the orthophotos of a natural event and outperformed E3D in simulating rill formation. Accurate rill formation and distribution modeling is important for planning and analyzing countermeasures against flooding and erosion, such as deriving nature-based solutions (e.g., agroforestry). The quantitative results of the uncalibrated HydroAS GS–Govers model indicated accurate sheet erosion quantity estimations compared to RUSLE2, and plausible estimations for small rills compared to observed data. However, erosion in large rills was often underestimated. This is consistent with conditions used in Govers (1990) experiments, at shallow water depths. For larger rills, calibration improved accuracy and demonstrated that observed data could be approximately simulated through parameter adjustment. However, calibration factors, such as soil properties, precipitation intensity, or quantity, needs to be investigated in more detail in order to improve the understanding of their influences.

Sensitivity analysis showed that grid resolution was a significant factor in determining erosion quantity, especially for small rills.

Unlike other models, such as EUROSEM and WEPP, this approach does not limit transport capacity based on the sediment load of the discharge. As the modeling results showed an underestimation of erosion compared to the measured data, the approach did not indicate any further limitations on the erosion rates.

The proposed method used a simple erosion approach to estimate the minimum erosion of croplands for a single heavy precipitation event. However, this approach should be enhanced by additional parameters and processes such as infiltration. It is also important to note that further erosion resulting from discharge pathways, such as at the wayside of a road and subsequent undercutting, was outside the scope of this study.

Acknowledgements The authors thank Prof. Dr. Jochen Kubiniok for his support regarding the theoretical approach of this study and Dr. Eva Loch for implementing the Govers approach in HydroAS.

Author Contributions Conceptualization: Rebecca Hinsberger and Alpaslan Yörük; Funding acquisition: Alpaslan Yörük; Methodology: Rebecca Hinsberger; Investigation: Rebecca Hinsberger; Software: Rebecca Hinsberger and Alpaslan Yörük; Supervision: Alpaslan Yörük; Writing – initial draft: Rebecca Hinsberger; Writing – reviewing and editing: Rebecca Hinsberger and Alpaslan Yörük.

Funding Open Access funding enabled and organized by Projekt DEAL. This study was financially supported by the Ministry of Environment, Saarland, Germany (Project SEROMO).

Data Availability The data supporting the findings of this study are available in the referenced literature.

Declarations

Competing Interests This study led to the development of a new module for soil erosion simulation in the hydrodynamic numerical HydroAS model. The soil erosion approach is available in the literature and can be coupled with other models. The development and distribution of the HydroAS model is managed by Hydrotec Ingenieurgesellschaft mbH, where AY works as a managing director with business and financial interests. However, no financial benefit was gained from this study. The funders had no role in the study design, data collection, analysis, or interpretation, writing of the manuscript, or decision to publish the findings.

References

Ackers P, White WR (1973) Sediment transport: new approach and analysis. J Hydraul Div 99(11):2041–2060. https://doi.org/10.1061/JYCEAJ.0003791

Aigner D, Bollrich G (2015) Handbuch der Hydraulik für Wasserbau und Wasserwirtschaft, 1st ed.; Beuth Verlag GmbH: Berlin, Germany. ISBN 978-3-410-21341-3

Al-Fugara A, Mabdeh AN, Alayyash S, Khasawneh A (2023) Hydrological and hydrodynamic modeling for flash flood and embankment dam break scenario: hazard mapping of extreme storm events. Sustainability 15:1758. https://doi.org/10.3390/su15031758

Andualem TG, Hewa GA, Myers BR, Peters S, Boland J (2023) Erosion and sediment transport modeling: a systematic review. Land 12:1396. https://doi.org/10.3390/land12071396

Batista P (2025) A Lakatosian history of soil-erosion modelling as a scientific research programme. EGU Gen Assembly 2025 Vienna Austria 27 Apr–2 May 2025(EGU25–18554). https://doi.org/10.5194/egusphere-egu25-18554

Beasley D, Huggins L, Monke A (1980) ANSWERS: A model for watershed planning. Trans ASAE 23:938–0944. https://doi.org/10.13031/2013.34692

Biswas TR, Begam S, Dey S, Sen D (2021) Equilibrium approach for modeling erosional failure of granular dams. Phys Fluids 33:043306. https://doi.org/10.1063/5.0039140

Borelli P, Alewell C, Alvarez P et al (2021) Soil erosion modelling: a global review and statistical analysis. Sci Total Environ 780:146494. https://doi.org/10.1016/j.scitotenv.2021.146494

Brazier RE, Hutton CJ, Parsons AJ, Wainwright J (2011) Scaling Soil Erosion Models in Space and Time. In: Morgan RPC; Nearing MA (Ed.) (2011) Handbook of Erosion Modelling. John Wiley & Sons ISBN: 978-1-4051-9010-7, pp 289–312

Bundesministerium für Land- und Forstwirtschaft, Umwelt und Wasserwirtschaft (BMLFUW) and Österreichischer Wasser- und Abfallwirtschaftsverband (ÖWAV) (Ed.) (2011) Fließgewässermodellierung – Arbeitsbehelf Feststofftransport und Gewässermorphologie. AV+Astoria Druckzentrum GmbH, Wien

Chow VT (1959) Open-Channel hydraulics. McGraw-Hill Book Company, New York, NY, USA

Costabile P, Cea L, Barbaro G, Costanzo C, Llena M, Vericat D (2024) Evaluation of 2D hydrodynamic-based rainfall/runoff modelling for soil erosion assessment at a seasonal scale. J Hydrol 632:130778. https://doi.org/10.1016/j.jhydrol.2024.130778

De Roo APJ, Wesseling CG, Cremers NHDT, Offermans RJE, Ritsema CJ, Van Oostindie K (1994) LISEM: A new physically based hydrological and soil erosion model in a GIS-environment, theory and implementation. IAHS Publ No 224:439–448

Deutscher Wetterdienst (DWD) (2024) Wetter- und Klimalexikon. Starkregen. https://www.dwd.de/DE/service/lexikon/begriffe/S/Starkregen.html. Accessed 02 Aug 2024

Dugan I, Pereira P, Kisic I, Bogunovic I (2024) Temporal dynamics of soil erosion and nutrient loss in Croatian orchard: experimental insights into resilience mechanisms. Environ Process 11:53. https://doi.org/10.1007/s40710-024-00735-1

Engelund F, Hansen E (1967) A monograph on sediment transport in alluvial streams. teknisk forlag, Copenhagen

Ferguson RI (2021) Roughness calibration to improve flow predictions in coarse-bed streams. Water Resour Res 57:e2021WR029979. https://doi.org/10.1029/2021WR029979

García-Feal O, González-Cao J, Gómez-Gesteira M, Cea L, Domínguez JM, Formella A (2018) An accelerated tool for flood modelling based on Iber. Water 10:1459. https://doi.org/10.3390/w10101459

Gerlinger K (1997) Erosionsprozesse auf Lößboden: Experimente und Modellierung. Dissertation, Universität Fridericiana zu Karlsruhe (TH)

Govers G (1990) Empirical relationships for the transport capacity of overland flow. Erosion, Transport and Deposition Processes (Proceedings of the Jerusalem Workshop, March-April 1987). IAHS Publ. no. 189,1990

Govers G, Poesen J (1988) Assessment of the interrill and rill contributions to total soil loss from an upland field plot. Geomorphology 1(4):343–354. https://doi.org/10.1016/0169-555X(88)90006-2

Hinsberger R (2024) Analysis of heavy precipitation–induced rill erosion. Environ Earth Sci 83:354. https://doi.org/10.1007/s12665-024-11671-6

Hinsberger R, Biehler A, Yörük A (2022) Influence of water depth and slope on roughness—experiments and roughness approach for rain-on-grid modeling. Water 14:4017. https://doi.org/10.3390/w14244017

Hu X, Song L (2018) Hydrodynamic modeling of flash flood in mountain watersheds based on high-performance GPU computing. Nat Hazards 91:567–586. https://doi.org/10.1007/s11069-017-3141-7

Hu P, Lei Y, Han J, Cao Z, Liu H, He Z (2019) Computationally efficient modeling of hydro-sediment-morphodynamic processes using a hybrid local time step/global maximum time step. Adv Water Resour 127:26–38. https://doi.org/10.1016/j.advwatres.2019.03.006

Hu P, Ji A, Li W, Tang X, Xiao W, Cao Z (2025) Capacity and noncapacity sediment transport characteristics in the Overtopping-induced Dam-Breaching process. J Hydraul Eng 151(2):04025001. https://doi.org/10.1061/JHEND8.HYENG-13985

Huang W, Cao ZX, Qi WJ et al (2015) Full 2d hydrodynamic modelling of rainfall-induced flash floods. J Mt Sci 12:1203–1218. https://doi.org/10.1007/s11629-015-3466-1

Huang R, Ni Y, Cao Z (2022) Coupled modeling of rainfall-induced floods and sediment transport at the catchment scale. Int J Sedim Res 37:715–728. https://doi.org/10.1016/j.ijsrc.2022.05.002

Huber A, Lumassegger S, Kohl B, Spira Y, Weingraber F, Achleitner S (2021) Modellierung pluvialer Sturzfluten – Anforderungen und Sensitivitäten der 2D-hydraulischenModellierung. Österr Wasser- und Abfallw 73:116–133. https://doi.org/10.1007/s00506-021-00749-1

Hydrotec (2025a) HydroAS, Reference manual, 2D-flow model for water management applications, version 6.2.5, Aachen. https://www.hydrotec.de/wp-content/uploads/HydroAS-Manual.pdf. Accessed 28 July 2025

Hydrotec (2025b) HydroAS FT, Reference manual, Add-ons for simulating sediment transport, version 6.2.5, Aachen. https://www.hydrotec.de/wp-content/uploads/HydroAS-Sedimenttransport-Manual.pdf. Accessed 28 July 2025

Hydrotec (2025c) HydroAS RiverMesh, User manual, Extension for the generation of a river channel for 2D modeling, version 2.2.1, Aachen. https://www.hydrotec.de/wp-content/uploads/HydroAS-RiverMesh-Manual.pdf. Accessed 28 July 2025

IPCC (2021) Summary for Policymakers. In: Climate Change 2021: The Physical Science Basis. Contribution of Working Group I to the Sixth Assessment Report of the Intergovernmental Panel on Climate Change; Masson-Delmotte, V., Zhai, P., Pirani, A., Connors, S.L., Péan, C., Berger, S., Caud, N., Chen, Y., Goldfarb, L., Gomis, M.I., Eds.; Cambridge University Press: Cambridge, UK and New York, NY, USA, 3–32. https://doi.org/10.1017/9781009157896.001

Jia Y, Wells RR, Momm HG, Zhang Y, Bennett SJ (2023) Physically based numerical model for the landscape evolution of soil-mantled watersheds driven by rainfall and overland flow. J Hydrol 620:129419. https://doi.org/10.1016/j.jhydrol.2023.129419

Kilinc M, Richardson EV (1973) Mechanics of soil erosion from overland flow generated by simulated rainfall. Hydrology Papers, no. 63, Colorado State University, Fort Collins, Colorado. http://hdl.handle.net/10217/61574

Laflen JM, Lane LJ, Foster GR (1991) WEPP: a new generation of erosion prediction technology. J Soil Water Conserv 46:34–38

Lavoie B, Mahdi TF (2017) Comparison of two-dimensional flood propagation models: SRH-2D and Hydro_AS-2D. Nat Hazards 86:1207–1222. https://doi.org/10.1007/s11069-016-2737-7

Liang Q, Xia X, Hou J (2016) Catchment-scale high-resolution flash flood simulation using the GPU-based technology. Procedia Eng 154:975–981. https://doi.org/10.1016/j.proeng.2016.07.585

LUBW Landesanstalt für Umwelt, Messungen und Naturschutz Baden-Württemberg, Publ. Anhänge 1 a, b, c zum Leitfaden, Kommunales Starkregenrisikomanagement in Baden-Württemberg (2020) Available online: https://pudi.lubw.de/detailseite/-/publication/47871. Accessed 10 Sep 2024

Meyer-Peter E, Müller R (1948) Formulas for Bed-Load Transport. International Association for Hydraulic Structures Research, Second Meeting, 7. – 9.06.1948, Stockholm

Morgan RPC, Quinton JN, Smith RE, Govers G, Poesen JWA, Auerswald K, Chisci G, Torri D, Styczen ME (1998a) The European soil erosion model (EUROSEM): a process-based approach for predicting soil loss from fields and small catchments. Earth Surf Process Land 23:527–544. https://doi.org/10.1002/(SICI)1096-9837(199806)23:6%3C;527::AID-ESP868%3E;3.0.CO;2-5

Morgan RPC, Quinton JN, Smith RE, Govers G, Poesen JWA, Auerswald K, Chisci G, Torri D, Styczen ME, Folly AJV (1998b) The European soil erosion model (EUROSEM): Documentation and user guide. Version 3.6. Silsoe College, Cranfield University

Nunes JP, Nearing MA (2011) Modelling Impacts of Climate Change: Case Studies using the New Generation of Erosion Models. In: Morgan RPC, Nearing MA (Ed.) (2011) Handbook of Erosion Modelling. John Wiley & Sons ISBN: 978-1-4051-9010-7, pp 289–312

Parkin GW, Gardner WH, Auerswald K (2008) Water erosion. In: Chesworth W (ed) Encyclopedia of soil science. Encyclopedia of Earth Sciences Series. Springer, Dordrecht. https://doi.org/10.1007/978-1-4020-3995-9_625

Quan X, He J, Cai Q, Sun L, Li X, Wang S (2020) Soil erosion and deposition characteristics of slope surfaces for two loess soils using indoor simulated rainfall experiment. Soil Till Res 204:104714. https://doi.org/10.1016/j.still.2020.104714

Sanz-Ramos M, Bladé E, González-Escalona F, Olivares G, Aragón-Hernández JL (2021) Interpreting the manning roughness coefficient in overland flow simulations with coupled hydrological-hydraulic distributed models. Water 13:3433. https://doi.org/10.3390/w13233433

Scherer U, Zehe E, Träbing K, Gerlinger K (2012) Prediction of soil detachment in agricultural loess catchments: model development and parameterization. CATENA 90:63–75. https://doi.org/10.1016/j.catena.2011.11.003

Semwal P, Khobragade SD, Nainwal HC (2017) Modelling of recent erosion rates in a lake catchment in the North-Western Siwalik Himalayas. Environ Process 4:355–374. https://doi.org/10.1007/s40710-017-0234-y

Smith RE, Goodrich DC, Unkrich CL (1999) Simulation of selected events on the Catsop catchment by KINEROS2 A report for the GCTE conference on catchment scale erosion models. Catena, 37, pp. 457–475. https://doi.org/10.1016/S0341-8162(99)00033-8

Wainwright J, Parsons AJ, Cooper JR, Gao P, Gillies JA, Mao L, Orford JD, Knight PG (2015) The concept of transport capacity in geomorphology. Rev Geophys 53:1155–1202. https://doi.org/10.1002/2014RG000474

Wang S, Flanagan DC, Engel BA (2019) Estimating sediment transport capacity for overland flow. J Hydrol. https://doi.org/10.1016/j.jhydrol.2019.123985

Wischmeier WH, Smith DD (1978) Predicting rainfall erosion losses. Agric Handb No 537:285–291. https://doi.org/10.1029/TR039i002p00285

Wu J, Hu P, Zhao Z, Lin Y-T, He Z (2023) A GPU-accelerated and LTS-based 2d hydrodynamic model for the simulation of rainfall-runoff processes. J Hydrol 623:129735. https://doi.org/10.1016/j.jhydrol.2023.129735

Yalin MS (1963) An expression for bed-load transportation. J Hydraul Div 89(3):221–250. https://doi.org/10.1061/JYCEAJ.0000874

Yörük A, Sacher H (2014) Methoden und Qualität von Modellrechnungen für HW-Gefahrenkarten. In Technische Universität Dresden, Institut für Wasserbau und technische Hydromechanik (Ed.): Simulationsverfahren und Modelle für Wasserbau und Wasserwirtschaft. Dresdner Wasserbauliche Mitt. 2014, 50, pp 55–64

Authors and Affiliations

Rebecca Hinsberger[1,2] · Alpaslan Yörük[2,3]

✉ Rebecca Hinsberger
rebecca.hinsberger@uni-saarland.de

[1] Physical Geography and Environmental Research, Saarland University, Saarbrücken, Germany

[2] Hydraulic Engineering and Water Management, School of Architecture and Civil Engineering, University of Applied Sciences, Saarbrücken, Germany

[3] Hydrotec GmbH, Engineering Company for Water and Environment, Aachen, Germany